State-of-Charge Estimation for Lithium-ion Battery Pack Using Reconstructed Open-Circuit-Voltage Curve

Chang Yoon Chun, Gab-Su Seo, Sung Hyun Yoon, and Bo-Hyung Cho
Department of Electrical and Computer Engineering
Seoul National University
Seoul, Republic of Korea
wobniw77@snu.ac.kr, bhcho@snu.ac.kr

***Abstract*— This paper proposes a state-of-charge (SOC) estimation algorithm for a series-connected Li-ion battery pack using a reconstructed open-circuit-voltage (OCV) curve. This method redefines the OCV-SOC relationship based on a cell which has the lowest available capacity and estimates the battery pack SOC and capacity information regardless of the type and existence of balancing circuit. To validate the performance of the proposed estimation method, a constant current profile is used for seven 18650 series-connected Li-ion batteries (7S1P). The experimental results verify the performance of the proposed battery pack SOC estimation algorithm.**

Keywords—battery pack; pack capacity; reconstructed open-circuit-voltage (OCV); state-of-charge (SOC).

I. INTRODUCTION

In estimating state-of-charge (SOC) of a Li-ion battery pack with series-connected cells, conventional pack model-based methods experience difficulties providing accurate battery status since they assume all batteries of a pack have the identical characteristics. Even though a screening process may improve the uniformity issue [1]-[3], the cell voltage variations in a pack are still inevitable even in the screened case. Due to unavoidable mismatches resulting from product tolerance and different capacity degradation of individual cells in use [4], it is challenging to estimate accurate battery status.

To overcome the inherent limitations of the pack model-based methods, cell model-based methods have been presented. They use the lowest voltage cell model [5] or averaged cell model [6]-[8] to achieve high estimation accuracy. By utilizing an additional SOC calibration process, the alternative methods obtain better performance. However, although they correct the estimation results considering the cell voltage variances, to achieve high estimation accuracy is still challenging since the battery pack SOC is not determined by a cell with the minimum voltage but by that with the minimum available energy.

The proposed SOC estimation algorithm locates the dominant cell which determines the entire battery pack capacity and SOC. Considering the dominant cell characteristic, the relation of open-circuit-voltage (OCV) and SOC is reconstructed. As a result, this method is able to accomplish the SOC estimation of a battery pack regardless of existence and type of balancing circuit with simple calculation. This paper is organized as follows. Section II presents discussions on battery pack capacity and pack SOC and the key idea of the SOC estimation algorithm. In Section III, the developed battery pack SOC estimation algorithm is validated using a constant current profile with seven 18650 series-connected Li-ion batteries (7S1P).

II. BATTERY PACK SOC ESTIMATION ALGORITHM

A. Capacity and SOC of a Packed Battery

The definition of the battery pack capacity was introduced in [6]-[7]. The battery pack capacity C_{pack} is expressed as

$$C_{\text{pack}} = \begin{cases} \min(SOC_i \cdot C_i) + \min((1-SOC_j)\cdot C_j) & \text{w/o balancing} \\ \min(C_i) & \text{Passive balancing} \\ \text{mean}(C_i) & \text{Active balancing} \end{cases} \quad (1)$$

where SOC_i and C_i are the SOC and capacity of i-th cell in the series-connected battery pack. As (1) describes, the existence and type of the balancing circuit determine the battery pack capacity.

In the balancing circuit-less case, the remaining capacity of a pack is clearly related to that of the lowest remaining capacity cell, $\min(SOC_i \cdot C_i)$, while the chargeable capacity is to one with the smallest chargeable room, $\min((1-SOC_j)C_j)$. If the voltage of the lowest remaining capacity cell (C1) at the moment when the lowest chargeable capacity cell (C2) reaches its upper limit is set as the new upper limit, the newly constructed OCV-SOC curve of C1 would represent the pack SOC.

Every ideally balanced cell in the pack has same chargeable room when the battery pack is charging. This means that C1 and C2 refer to the same cell, and this cell has the lowest cell capacity in the pack. For this reason, the battery pack capacity equals to the minimum cell capacity at passive balancing, and the averaged capacity

978-1-4799-2705-0/14/$31.00 ©2014 IEEE

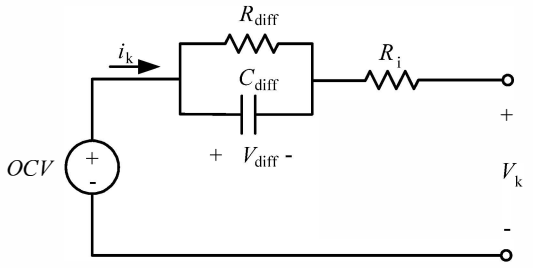

Fig. 1. Battery Thevenin equivalent circuit model.

TABLE I
BATTERY CHARACTERISTICS

Symbol	Meaning	Value
R_i	Series resistance	0.1695 Ω
R_{diff}	Diffusion resistance	0.0249 Ω
C_{diff}	Diffusion capacitance	7000 F

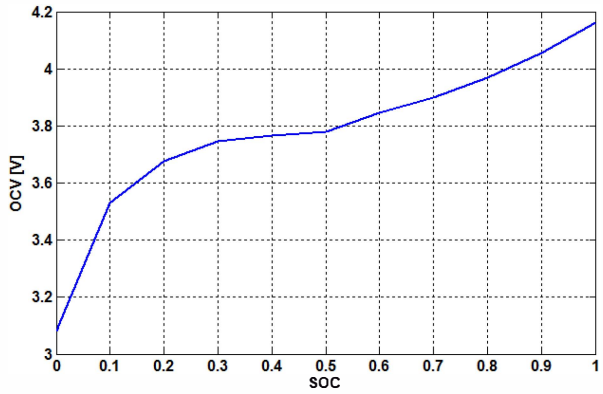

Fig. 2. OCV-SOC curve of a typical 18650 Li-ion battery.

of the entire pack at active balancing because all the cells are adjusted to have same SOC state. According to the relations, it is noted that the status of C1 represents the pack capacity regardless of the type and existence of balancing. As a result, battery pack SOC is derived as

$$SOC_{pack} = \frac{\min(SOC_i \cdot C_i)}{C_{pack}} = \frac{SOC_{C1} \cdot C_{C1}}{\alpha \cdot C_{C1}} \quad (2)$$

where α is the calibration factor which is the capacity ratio coefficient of the newly constructed OCV-SOC curve.

B. Battery Cell Model and OCV Curve Reconstruction

Fig. 1 shows a Thevenin equivalent circuit model for a single battery cell, and Table I presents the characteristic values of a 18650 Li-ion battery including a series resistor (R_i), a R-C branch (R_{diff} and C_{diff}). Fig. 2 illustrates SOC and OCV relationship. As aging proceeds in a battery cell, the battery impedance tends to increase, which leads to the limited available OCV range due to the increased internal energy loss. As another result of aging, the battery capacity also decreases. Since the high internal impedance and the low capacity cause higher and lower cell voltage in charging and discharging, respectively, it limits operating range of the cell and battery pack.

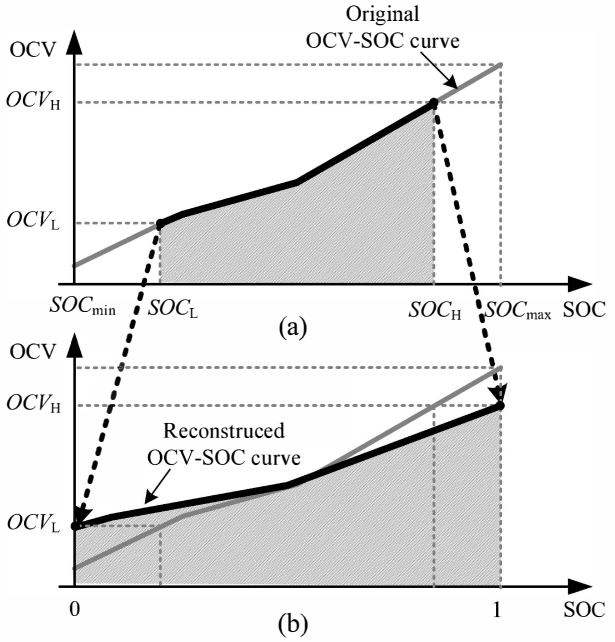

Fig. 3. OCV-SOC curve reconstruction: (a) original OCV-SOC curve with upper and lower boundary identified, (b) reconstructed battery OCV-SOC curve.

This paper uses OCV information for SOC estimation. As demonstrated in Fig. 3, the lowest OCV, OCV_L, is obtained through calculation or measurement with sufficient rest time when the voltage of the lowest remaining capacity cell (C1) meets lower cutoff voltage. The highest OCV value of the lowest remaining capacity cell (C1), OCV_H, is obtained when any cell voltage, which would be the voltage of C1 or not, meets its upper limit. From the OCV-SOC relationship, SOC_H and SOC_L is obtained, and calibration factor α is simply derived from

$$\alpha = \frac{(SOC_H - SOC_L)}{(SOC_{max} - SOC_{min})}. \quad (3)$$

The OCV operating range is reconstructed like the dotted line in Fig. 3(a), and (b).

The relationship between the lowest remaining capacity cell SOC, SOC_k, and the battery pack SOC, SOC_{pack}, can be defined as

$$SOC_{pack} = \begin{cases} 0, & SOC_{pack} \le 0 \\ \frac{1}{\alpha}(SOC_k - SOC_L) = \frac{(SOC_k - SOC_L)}{(SOC_H - SOC_L)}. \\ 1, & SOC_{pack} \ge 1 \end{cases} \quad (4)$$

In (4), the battery pack SOC is trimmed not to exceed its upper (100%) and lower (0%) boundary.

C. Proposed Battery Pack SOC Estimation

As illustrated in Fig. 4, when the BMS starts its operation, the lowest remaining capacity cell (C1), which has the dominant characteristic, is not identified yet. In the initial operation, the system selects a cell which shows the highest voltage in charging or the lowest in

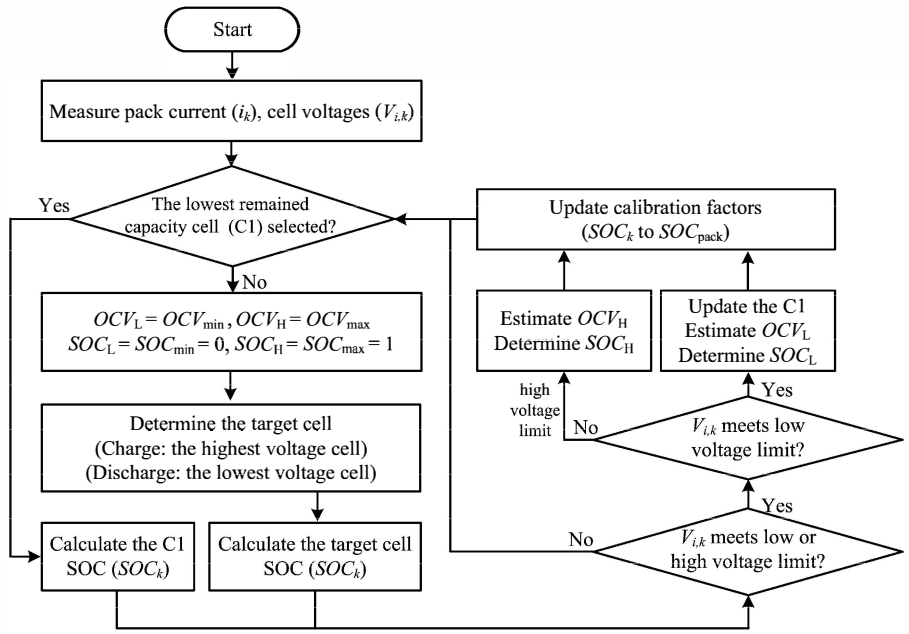

Fig. 4. Flowchart for the calibration factors derivation.

discharging, and lets the cell SOC to represent the pack SOC until C1 is located. OCV_H, OCV_L, SOC_H, and SOC_L are set to the initial values. Because no correction is applied in this state, SOC estimation error would occur.

If a battery voltage of a cell reaches its lowest limit during operation, it is selected as the dominant cell C1 and the BMS sets the OCV of C1 as OCV_L. The SOC estimation algorithm estimates the pack SOC based on the dominant cell characteristic and operating condition. On the other hand, if a battery voltage of a cell reaches its highest limit, it sets the OCV of the cell as OCV_H while the dominant cell is not updated. The management system continuously updates C1 as the min(SOC_i·C_i), and proceeds the same SOC estimation and updating processes, as shown in Fig. 4.

D. Extended Kalman Filter Algorithm

The extended Kalman filter (EKF) is used to estimate the SOC in many literatures [9]-[11]. The process model and the measurement model, expressed as

$$x_k = \begin{bmatrix} SOC_{k+1} \\ V_{\text{diff},k+1} \end{bmatrix} = \begin{bmatrix} 1 & 0 \\ 0 & 1-\dfrac{\Delta t}{R_{\text{diff}} C_{\text{diff}}} \end{bmatrix} \begin{bmatrix} SOC_k \\ V_{\text{diff},k} \end{bmatrix} + \begin{bmatrix} -\dfrac{\Delta t}{C_{\text{C1}}} \\ \dfrac{\Delta t}{C_{\text{diff}}} \end{bmatrix} i_k \tag{5}$$

$$V_k = h_k(\text{OCV}, V_{\text{diff}}) - R_1 i_k = OCV(SOC_k) - V_{\text{diff}} - R_1 i_k, \tag{6}$$

defines the SOC and diffusion voltage between over the R-C branch and the estimated terminal cell voltage based on the battery model in Fig. 1. EKF ensures the SOC estimation is within a specified range even though initial error and measurement error occur. The specified range is determined by battery model, especially the OCV. Thus, if the OCV in battery model is more accurate, EKF algorithm guarantees reliable results. Otherwise, SOC information fluctuates in a certain bound.

In this paper, the proposed algorithm uses a reduced order EKF with a noise model and data rejection algorithm from [10].

III. VERIFICATION

In this section, the SOC estimation results for battery pack and the lowest remaining capacity cell are shown in detail. In order to verify the proposed method, a single pack of seven series-connected batteries (7S1P), which are Samsung SDI 2.6Ah 18650 Li-ion batteries, is used. Before the experiment, most of the cell voltages are balanced, and the initial cell voltages in the battery pack stay constant. The battery pack is charged under the constant current-constant voltage (CC-CV) protocol with 0.5 C rating and discharged under the same constant current conditions, and rested for 1.5 h, as shown in Fig. 5(a). For a single cell case, the voltage is held at 4.2 V till the current drops to 130 mA (0.05 C) at CC-CV and the low cutoff voltage is set to be 2.75V at discharging. However, for this battery pack case, 29.05-V/21-V (4.15 V, 3 V each cell) are assigned as the cutoff voltages for charging/discharging case in order to place the margin. In other words, even if the battery balancing circuit exists but the balancing speed is not sufficient, imbalance may occur between cells. For protecting battery cells in the pack, it is necessary to limit the operating range of the battery cells unlike the cell parameters extraction process.

Fig. 5(a) shows seven cell voltages in the battery pack when the battery pack is charging/discharging or rest, and Figs. 5(b), 5(c), 5(d) are the expanded waveforms of Fig. 5(a) at the notable mode changes for further discussions. In the beginning, the lowest remaining capacity cell (C1) is not found yet, the highest voltage cell is a target cell and the SOC of the target cell is estimated. While the charging progresses in Fig. 5(b), the cell #6 has the largest voltage variation. As, the voltage of cell #6 reaches the upper limit, the cell #6 is identified as the

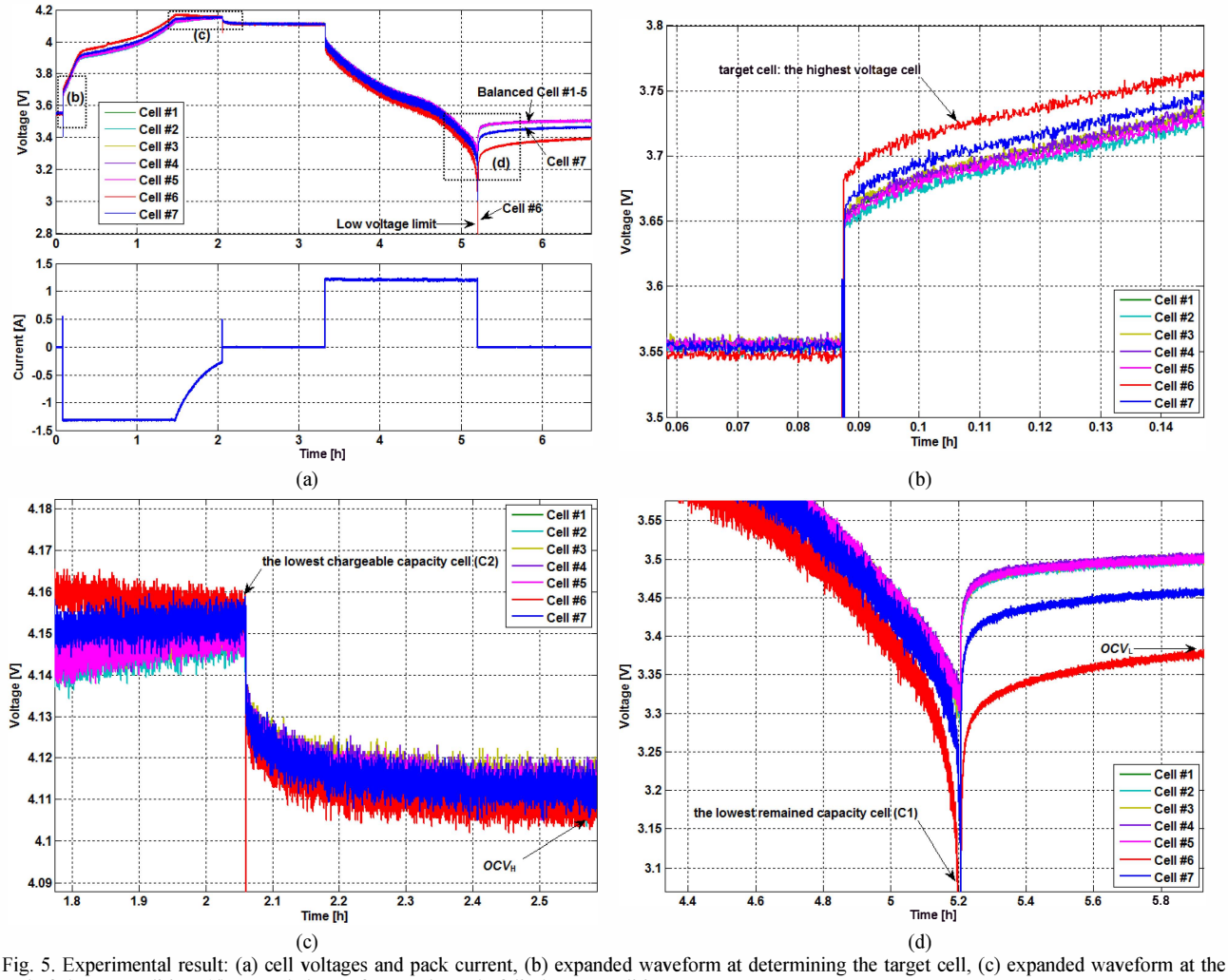

Fig. 5. Experimental result: (a) cell voltages and pack current, (b) expanded waveform at determining the target cell, (c) expanded waveform at the end of charge condition, (d) expanded waveform at the end of discharge condition.

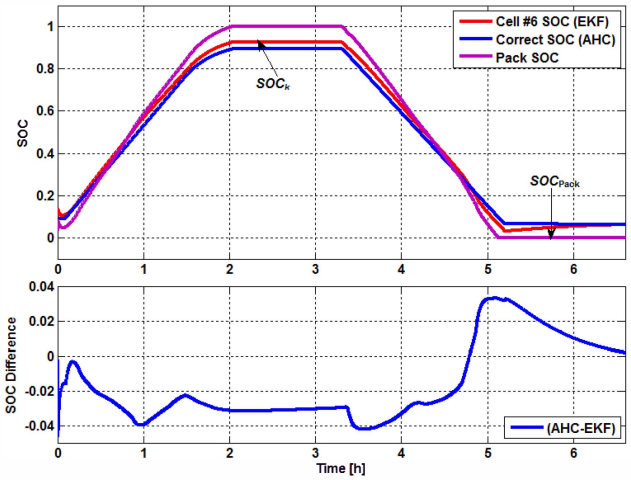

Fig. 6. Estimated SOC (cell # 6), battery pack SOC and SOC difference

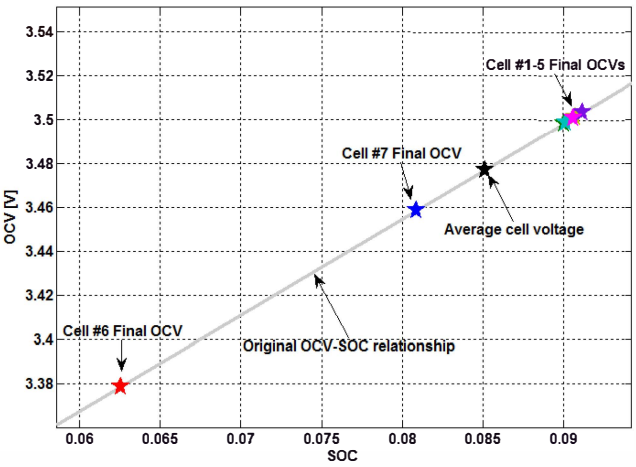

Fig. 7. Estimated OCV and SOC values using each cell model and average cell voltage model at SOC_{pack} =0.

lowest chargeable capacity cell (C2) as observed in Fig. 5(c) and the battery pack SOC reaches SOC_{max}. At last, discharging of the pack is halted as shown in Fig. 5(d) as the voltage of cell #6 reaches the lower limit. At the moment, cell #6 is the lowest remaining capacity cell (C1), and the battery pack SOC reaches SOC_{min}. The SOCs of the C1 and the pack are calculated using the original OCV curve, as shown in Fig. 2, and the updating calibration factors from (3). As a result, the pack capacity comes from the lowest remaining capacity cell (C1) and calibration factor, and the final battery pack SOC is obtained as shown in Fig. 6.

The Fig. 7 is the enlarged version of Fig. 2 in which OCV distribution at the end of discharging is projected on the low SOC range curve. At the beginning of the experiment, all initial OCVs are placed around 9% SOC in Fig. 5. However, the final SOC values are placed on 6.2% to 9% depending on the voltage of the each cell distribution. This slight SOC difference comes from its OCV difference and these results indicate that if the battery pack SOC estimation is based on other cell model or averaged cell model, the SOC estimation error should be larger than the proposed method due to their model error.

IV. CONCLUSIONS

In this paper, a battery pack SOC estimation algorithm is proposed which uses the dominant cell characteristic. The proposed method reconstructs the OCV-SOC relationship based on the lowest available capacity cell since it determines the battery pack SOC regardless of the type and existence of balancing. With the updated calibration factors, the newly defined OCV-SOC relationship allows the battery management system (BMS) to improve its SOC estimate performance.

ACKNOWLEDGMENT

This work was partly supported by the Technological Innovation R&D program (S2058100) funded by the Small and Medium Business Administration (SMBA, Korea); the Human Resources Development program (No. 20124030200030) of the Korea Institute of Energy Technology Evaluation and Planning (KETEP) grant funded by the Korea government Ministry of Trade, Industry and Energy; and the Seoul National University Research Grant.

REFERENCES

[1] J. Kim et al., "High accuracy state-of-charge estimation of Li-ion battery pack based on screening process," in *Proc. IEEE Appl. Power Electron. Conf. Expo. (APEC)*, 2011, pp. 1984-1991.

[2] J. Kim et al., "Stable configuration of a Li-ion series battery pack based on a screening process for improved voltage/SOC balancing," *IEEE Trans. Power Electron.*, vol. 27, no.1, pp. 411-424, 2012.

[3] R. Xiong, "Adaptive state of charge estimator for lithium-ion cells series battery pack in electric vehicles," *J. Power Sources*, vol. 242, pp. 699-713, 2013.

[4] M. Broussely et al., "Main aging mechanisms in Li ion batteries," *J. Power Sources*, vol. 146, pp. 90-96, 2005.

[5] X. Liu et al., "State-of-charge estimation for power Li-ion batteries pack using Vmin-EKF," in *Proc. IEEE Int. Conf. Software Eng. and Data Mining (SEDM)*, 2010, pp. 27-31.

[6] L. Zhong et al., "A method for the estimation of the battery pack state of charge based on in-pack cells uniformity analysis," *Appl. Energy*, vol. 113, pp. 558-564, 2014.

[7] Y. Zheng et al., "$LiFePO_4$ battery pack capacity estimation for electric vehicles based on charging cell voltage curve transformation," *J. Power Sources*, vol. 226, pp. 33-41, 2013.

[8] H. Dai et al., "Online cell SOC estimation of Li-ion battery packs using a dual time-scale Kalman filtering for EV applications," *Appl. Energy*, vol. 95, pp. 227-237, 2012.

[9] G. L. Plett, "Extended Kalman filtering for battery management systems of LiPB-based HEV battery packs: Part 1-3," *J. Power Sources*, vol. 134, pp. 252-292, 2004.

[10] O. Nam et al., "Li-ion battery SOC estimation method based on the reduced order extended Kalman filtering," in *Proc. 4th Int. Energy Convers. Eng. Conf. and Exhibit*, 2006, pp. 1-9.

[11] M. Charkhgard and M. Farrokhi, "State-of-charge estimation for lithium-ion batteries using neural networks and EKF," *IEEE Trans. Ind. Electron.*, vol. 57, no. 12, pp. 4178-4187, 2010.